

A Constitutive Model for Creep of Lead-Free Solders Undergoing Strain-Enhanced Microstructural Coarsening : A First Report

I. Dutta^{*}

Center for Materials Science and Engineering
Department of Mechanical Engineering
Naval Postgraduate School
Monterey, CA 93943

ABSTRACT

Lead-free solder joints in microelectronic applications frequently have microstructures comprising a dispersion of intermetallic particles in a Sn-matrix. During thermo-mechanical cycling of the solder joint, these particles undergo strain-enhanced coarsening, resulting in a continuously evolving creep behavior. Since the extent of coarsening is dependent on the stress/strain state, which is dependent on the location within a joint, it is important that creep models used in joint-life prediction incorporate these effects. Here, an approach for incorporating the effect of in-situ second-phase particle coarsening in a dislocation creep model applicable to lead-free solder alloys is proposed. The formulation, which can be expressed in a closed analytic form following some simplifications, incorporates the effects of both static and strain-enhanced coarsening, and can be easily incorporated in current finite-element codes for joint behavior simulation.

^{*} Professor, Center for Materials Science and Engineering, Department of Mechanical Engineering, Naval Postgraduate School, Monterey, CA 93943; idutta@nps.navy.mil.

1. INTRODUCTION

Microelectronic solder joints are typically exposed to aggressive thermo-mechanical cycling (TMC) conditions with high homologous temperatures and large strain ranges during service. During prolonged TMC, the microstructures of solder joints can undergo rapid strain-enhanced coarsening. Since solder joint life is dictated largely by the creep strain range, which may be influenced appreciably by microstructural scale, it is important to develop new constitutive models for solder creep incorporating the effect of microstructural coarsening, which can then be incorporated in finite element models (FEM) for accurate predictions of joint reliability.

An example of phase coarsening in a flip-chip joint of lead-free solder (Sn-4.7%Ag-1.7%Cu) is shown in Figure 1, which shows that the fine Ag_3Sn particles dispersed in the Sn-rich matrix coarsen appreciably within 200 thermo-mechanical cycles, and dramatically by 1200 cycles, with commensurate increases in the inter-particle spacing. As shown in the size distribution histograms in Figure 2, the average size of the approximately spherical Ag_3Sn particles grows from $0.35\mu\text{m}$ to $1\mu\text{m}$ during the first 200 cycles, with platelets of average length $\sim 2.5\mu\text{m}$ developing by 1200 cycles. The coarser Cu_6Sn_5 particles also grow, but at a much slower rate.

The phenomenon of phase coarsening during TMC has been widely studied for Sn-Pb solders [1-8], and attempts have been made to incorporate coarsening effects into creep models for use in joint life prediction [5-8]. Two approaches have been adopted. In the first, the empirical dependence of the microstructural scale on the number of elapsed cycles (v_c) during TMC is experimentally determined, and then this is used with the relevant creep equation to compute the creep strain, and thence the solder life [4,5]. However, since the microstructural scale actually depends on several parameters besides v_c (such as strain range, rate, etc.), the applicability of this approach is limited. In a more rigorous approach, the instantaneous grain size (d) is first computed using an appropriate coarsening kinetics law during a step-wise solution scheme such as FEM, and is then utilized to update the creep law [6,7]. However, this approach is complex in its execution

scheme because of the absence of a closed-form creep law incorporating coarsening, and as a result, has not been widely implemented.

Additionally, to date, all creep studies incorporating phase coarsening have been based on Pb-Sn solders. However, the mechanism of microstructural coarsening, and the way coarsening is expected to affect the creep behavior of Pb-free solders (such as Sn-Ag, Sn-Ag-Cu or Sn-Cu) are fundamentally different from Pb-Sn solders. The microstructure of Pb-Sn solders in typical microelectronic joints consists of equiaxed grains of Pb-rich and Sn-rich phases, both of which coarsen. This affects the *diffusional creep* component only, with no effect on dislocation creep. Contrarily, the microstructure of Sn-Ag, Sn-Ag-Cu or Sn-Cu solders typically consist of dispersed intermetallics in a β -Sn matrix, the grain size of which is considerable relative to the joint size (a typical flip-chip solder joint may contain only a few grains). This minimizes the impact of diffusional creep. The primary coarsening effect in these solders, therefore, arises from the rapid coarsening of the finely dispersed intermetallic particles, which is likely to affect the *dislocation creep* component.

This paper reports on an approach for explicitly incorporating second phase particle coarsening into a closed-form dislocation creep law for typical lead-free solder microstructures used in microelectronics.

2. APPROACH

2.1. Microstructure

The starting microstructure is assumed to be similar to that shown in Figure 1a, with a dispersion of fine intermetallic particles in a β -Sn matrix. The coarsening of only one precipitate type (e.g., Ag_3Sn in eutectic Sn-Ag solder) is considered. It is assumed that the joint size is small in relation to the matrix grain size, so that a typical joint contains a relatively small number of grains, allowing the contribution of diffusional creep and associated grain size effects to be ignored.

2.2. Creep Model Selection

Most creep formulations for dispersion-strengthened high strength materials contain a threshold stress term and are based on observations of anomalously high values of stress exponent (n) and activation energy (Q) [9], none of which are common in lead-free solders [10-12]. Therefore, typical creep equations for dispersion-strengthened alloys are not applicable to lead-free solders. Accordingly, the only available dislocation creep equation for a dispersion-containing alloy with an explicit microstructural scale parameter [13] is chosen as the starting point.* The model assumes that the rate-controlling process is climb (and eventual annihilation) of dislocation segments over second phase particles, and is consistent with n and Q values expected for the matrix alloy. The model may be expressed as:

$$\dot{\epsilon} = A \left(\frac{Gb}{kT} \right) \left(\frac{\lambda^2}{d_p} \right) \left(\frac{\sigma}{G} \right)^n D_{\text{eff}} \quad (1)$$

where $\dot{\epsilon}$ is the quasi-steady state creep rate, G is the shear modulus, k is the Boltzmann's constant, T is the temperature, σ is the stress, λ is the inter-particle spacing, d_p is the particle size, and D_{eff} is the effective self-diffusivity of Sn in the solder matrix. In order to make equation 1 applicable over a larger range of stresses, we may re-write it as:

$$\dot{\epsilon} = A_1 \left(\frac{Gb}{kT} \right) \left(\frac{\lambda^2}{d_p} \right) \left[\sinh \left(\frac{\alpha \sigma}{G} \right) \right]^n D_{\text{eff}} \quad (2)$$

where α is the power-law breakdown parameter. Assuming that the microstructure contains a uniform distribution of particles of a fixed volume fraction V_f (obtainable directly from the phase diagram), the parameter (λ^2/d) may be rewritten as :

$$\frac{\lambda^2}{d_p} = A_2 \frac{r}{V_f^{2/3}} = A_2' r \quad (3)$$

where r is the particle radius, A_2 is a geometrical constant, and A_2' depends on geometry and the alloy phase constitution. Combining equations 2 and 3, we have:

$$\dot{\epsilon} = A_3 \left(\frac{Gb}{kT} \right) r \left[\sinh \left(\frac{\alpha \sigma}{G} \right) \right]^n D_{\text{eff}} \quad (4)$$

* The applicability of this model to lead-free solders has not been verified experimentally. It is used here mainly to develop the approach, which can be adapted in the future to a suitable creep law containing an appropriate microstructural scale term. Ongoing work is addressing this.

During TMC, the particle size r increases due to both static and dynamic coarsening. It is well known that phase coarsening may be greatly accelerated when deformation is superimposed on temperature, because of enhanced diffusion due to the increased vacancy concentration induced by plasticity [14,15]. The term r in equation 4 therefore needs to be replaced by an appropriate stress/strain history dependent function, in order to incorporate the effect of microstructural coarsening into the dislocation creep equation.

2.3. Creep with Coarsening Particles

Accelerated microstructural coarsening during thermo-mechanical deformation is attributable to the generation of excess vacancies due to the combined effect of (i) the local hydrostatic stress state (σ_h), and (ii) the instantaneous inelastic strain rate ($\dot{\epsilon}$). In general, a greater tensile σ_h and a higher $\dot{\epsilon}$ enhance the local vacancy concentration in the solder, thereby augmenting the diffusive flux and hence the coarsening kinetics. In the following, the functional dependency of the particle size r on σ_h and $\dot{\epsilon}$ are derived.

The total vacancy concentration at any location within the solder joint at any instant t may be written as the sum of the equilibrium vacancy concentration and that due to the applied instantaneous strain rate:

$$n_{\text{total}} = n_{\text{eqlm}} + n_{\text{strn}} \quad (5)$$

$$\text{where } n_{\text{eqlm}} = \exp\left(-\frac{Q_{f,v}}{kT}\right) \exp\left(\frac{\sigma_h \Omega}{kT}\right), \text{ and} \quad (6)$$

$$n_{\text{strn}} = \exp\left(-\frac{Q_{f,v}}{kT}\right) \exp\left(\frac{\sigma_h \Omega}{kT}\right) N \dot{\epsilon} \left[1 - \exp\left(-\frac{t}{\tau_c}\right)\right] \quad (7)$$

Here $Q_{f,v}$ is the enthalpy of formation of a vacancy, Ω is the atomic volume, σ_h is the hydrostatic stress at that location, τ_c is a time constant associated with the decay of a vacancy following formation, and N is a constant which scales the vacancy concentration to $\dot{\epsilon}$. Equations 6 and 7 are similar to those proposed in reference 14, but are modified to account for the hydrostatic stress component, which has been observed to play an appreciable role in phase coarsening in solders [16]. Based on the Lifshitz-Wagner theory [17,18], the coarsening rate of second phase particles may be written as:

$$\frac{dr}{dt} = \frac{B_1 \gamma_s V_m C_o}{3r^2 RT} K_2 n_{\text{total}} \quad (8)$$

where B_1 is a constant, γ_s is the specific energy of the particle-matrix interface, V_m is the molar volume of the second phase, C_o is the equilibrium solute concentration in the matrix, and K_2 is given by :

$$K_2 = D_{\text{sol}}/n_{\text{eqm}} = D_{\text{sol}}^0 \exp\left[-(Q_{\text{sol}} - Q_{f,v})/kT\right] \quad (9)$$

where D_{sol} is the effective solute diffusivity in the matrix, and D_{sol}^0 and Q_{sol} are the associated frequency factor and activation energy. Combining equations 5 through 9, one gets, for the deformation state dependent particle size:

$$3r^2 \frac{dr}{dt} = \frac{B_1 \gamma_s V_m C_o}{RT} D_{\text{sol}} \exp\left(\frac{\sigma_h \Omega}{kT}\right) \left[1 + N \dot{\epsilon} \left(1 - e^{-\frac{t}{\tau_c}}\right)\right] \quad (10)$$

Now, the particle size r at any time $t + \Delta t$ may be represented as:

$$r(t + \Delta t) = r(t) + \Delta r \quad (11)$$

where $r(t)$ is the particle radius at time t , and Δr is the particle size increment during a time increment Δt . $r(t)$ equals the initial particle size r_o at the beginning of the thermal excursion ($t=0$), and is updated after every solution step in a step-wise solution scheme. Based on equations 11 and 4, we can write for the creep rate at time $t + \Delta t$:

$$\dot{\epsilon}(t + \Delta t) = \dot{\epsilon}(t) + \Delta \dot{\epsilon} = A' [r(t) + \Delta r] \quad (12)$$

where $\dot{\epsilon}(t)$ is the strain rate at time t , $\Delta \dot{\epsilon}$ is the incremental contribution of Δr to the strain rate, and the parameter A' includes all the terms on the right hand side of equation 4 except r . In a step-wise solution scheme, where T and t are incrementally altered, $\Delta \dot{\epsilon}$ is computed at every time increment Δt , and added to the previous value of $\dot{\epsilon}(t)$ according to equation 12 (starting from $t=0$) to obtain the prevailing value of the creep rate $\dot{\epsilon}(t + \Delta t)$. At $t=0$ and $T=T_{\text{start}}$, when $r=r_o$, the strain rate $\dot{\epsilon}_o$ is given simply by:

$$\dot{\epsilon}(t = 0) = \dot{\epsilon}_o = A_3 \left(\frac{Gb}{kT_{\text{start}}}\right) r_o \left[\sinh\left(\frac{\alpha \sigma}{G}\right)\right]^n D_{\text{eff}} \quad (13)$$

To find $\Delta\dot{\epsilon}$, we integrate equation 10, and assuming that the radius increment Δr associated with the time increment Δt is small, and that the contribution of static annealing in this short time may be ignored, we obtain:

$$\Delta r = \left(\frac{B_1 \gamma_s V_m C_o}{RT} \right) \frac{D_{sol}}{3r_o^2} \exp \left(\frac{\sigma_h \Omega}{kT} \right) N \phi \dot{\gamma} \left[\Delta t + \tau_c e^{-\frac{\Delta t}{\tau_c}} \right] \quad (14)$$

and

$$\Delta\dot{\epsilon} = A_3 \left(\frac{Gb}{kT} \right) \left(\frac{B_1 \gamma_s V_m C_o}{RT} \right) \frac{D_{sol}}{3r_o^2} \exp \left(\frac{\sigma_h \Omega}{kT} \right) N \phi \dot{\gamma} \left[\Delta t + \tau_c e^{-\frac{\Delta t}{\tau_c}} \right] \left[\sinh \left(\frac{\alpha \sigma}{G} \right) \right]^n D_{eff} \quad (15)$$

where $\tau_c \approx L^2/(2D_v)$, D_v being the vacancy diffusivity and L being the mean distance traversed by a vacancy before being annihilated via absorption at a dislocation. Here the term $\dot{\epsilon}$ in equation 10 has been replaced by the term $\phi \dot{\gamma}$, where $\dot{\gamma}$ is the shear strain rate imposed on the solder joint during TMC*, and ϕ is a constant representing the fraction of $\dot{\gamma}$ which is inelastic. Since the temperature varies with time during TMC, T in equations 14 and 15 represent the mean temperature during the small time increment Δt . Thus, in a step-wise solution scheme, the instantaneous creep rate during the i^{th} solution step is obtained as $\dot{\epsilon}_i = \dot{\epsilon}_{i-1} + \Delta\dot{\epsilon}_i$, with $\Delta\dot{\epsilon}_i$ being given by equation 15.

2.4. A Simplified Solution

In solution-schemes where a step-wise updating of the creep equation by repeated recalculation of the history dependent term $\dot{\epsilon}(t)$ (i.e., $\dot{\epsilon}_{i-1}$) is cumbersome, an approximate closed-form solution may be derived. First, we represent the instantaneous particle radius as:

$$r(t + \Delta t) = r_o + r_{cum} + \Delta r \quad (16)$$

where r_{cum} is the cumulative increase in particle size from $t=0$ to $t=t$, such that $r(t) \approx r_o + r_{cum}$. The resultant creep rate may then be written as:

* For a flip-chip joint, $\dot{\gamma} = \frac{\Delta\alpha \Delta T \cdot x}{h \Delta t}$, where $\Delta\alpha$ is the difference in CTE between the chip and the substrate,

ΔT is the temperature range of TMC, x is the distance of the solder-joint from the mechanical neutral point (i.e., the center of the chip), h is the stand-off height (solder joint thickness), and Δt is the time associated with the temperature change ΔT .

$$\dot{\epsilon}(t + \Delta t) = \dot{\epsilon}_0 + \dot{\epsilon}_{\text{cum}} + \Delta \dot{\epsilon} = A' [r_0 + r_{\text{cum}} + \Delta r] \quad (17)$$

where $\dot{\epsilon}_0$ and $\Delta \dot{\epsilon}$ (i.e., r_0 and Δr) are computed as before.

We may find $\dot{\epsilon}_{\text{cum}}$ (or r_{cum}) by integrating equation 10, and by assuming that (i) the cumulative elapsed time $t \gg \tau_c$, and (ii) the term $\dot{\epsilon} \cdot t$, representing the inelastic strain accumulated during time t may be approximated as $2\dot{\gamma} t_{\text{hc}} v_c \phi$, which gives the cumulative shear strain during v_c TMCs, each with a half-period of t_{hc} . Here, $\dot{\gamma}$ is the average shear strain rate during a half cycle, and is given by $\dot{\gamma} \approx \frac{\Delta \alpha (T_{\text{max}} - T_{\text{min}})}{h t_{\text{hc}}}$, where

$(T_{\text{max}} - T_{\text{min}})$ is the temperature range of the cycle. This gives:

$$r_{\text{cum}} = \left[\left(\frac{B_1 \gamma_s V_m C_o}{RT} \right) \bar{D}_{\text{sol}} (t + 2N\dot{\gamma} t_{\text{hc}} v_c \phi) + r_0^3 \right]^{1/3} - r_0 \quad (18)$$

and

$$\dot{\epsilon}_{\text{cum}} = A_3 \left(\frac{Gb}{kT} \right) \left\{ \left[\left(\frac{B_1 \gamma_s V_m C_o}{RT} \right) \bar{D}_{\text{sol}} (t + 2N\dot{\gamma} t_{\text{hc}} v_c \phi) + r_0^3 \right]^{1/3} - r_0 \right\} \left[\sinh \left(\frac{\alpha \sigma}{G} \right) \right]^n D_{\text{eff}} \quad (19)$$

where the term \bar{D}_{sol} represents the solute diffusivity averaged over the temperature range of the TMC (T_{min} to T_{max}), corresponding to a time period t_{hc} , and is given by:

$$\bar{D}_{\text{sol}} = \frac{\int_0^{t_{\text{hc}}} D_o^{\text{sol}} \exp \left[\left(\frac{\sigma_h \Omega}{k} - \frac{Q_{\text{sol}}}{R} \right) \frac{1}{T} \right] dt}{\int_0^{t_{\text{hc}}} dt} \quad (20)$$

For a linear time-dependence of temperature ($T = T_{\text{min}} + \beta t$) during TMC, this yields :

$$\bar{D}_{\text{sol}} = \frac{D_{\text{min}}}{t_{\text{hc}}} \frac{e^{a/4b}}{\sqrt{ab}} \frac{\sqrt{\pi}}{2} [\text{erf}(\eta_o) - \text{erf}(\eta_c)] \quad (21)$$

$$\text{where } D_{\text{min}} = D_o^{\text{sol}} \exp \left[\left(\frac{\sigma_h \Omega}{k} - \frac{Q_{\text{sol}}}{R} \right) \frac{1}{T_{\text{min}}} \right], \quad (22a)$$

$$a = - \left(\frac{\sigma_h \Omega}{k} - \frac{Q_{\text{sol}}}{R} \right) \frac{\beta}{T_{\text{min}}^2}, \quad b = \frac{\beta}{2 T_{\text{min}}}, \quad (22b)$$

$$\eta_o = \frac{\sqrt{ab}}{2b}, \quad \text{and} \quad \eta_c = \sqrt{ab} \left(\frac{1}{2b} - t_{hc} \right) \quad (22c)$$

Substituting for $\dot{\epsilon}_o$, $\Delta\dot{\epsilon}$ and $\dot{\epsilon}_{cum}$ in equation 17 using equations 13, 15 and 19, we have, for the total strain rate due to creep during any time interval Δt :

$$\dot{\epsilon} \cong A_3 \left(\frac{Gb}{kT} \right) \left[\sinh \left(\frac{\alpha\sigma}{G} \right) \right]^n D_{eff} \times \left\{ \left[\left(\frac{B_1 \gamma_s V_m C_o}{RT} \right) \bar{D}_{sol} (t + 2N \dot{\gamma} t_{hc} v_c \phi) + r_o^3 \right]^{1/3} + \left(\frac{B_1 \gamma_s V_m C_o}{RT} \right) \frac{D_{sol}}{3r_o^2} \exp \left(\frac{\sigma_h \Omega}{kT} \right) N \phi \dot{\gamma} \left[\Delta t + \tau_c e^{\frac{\Delta t}{\tau_c}} \right] \right\} \quad (23)$$

With progressive TMC, i.e., as the time t becomes large, Δr becomes small compared with r_{cum} (since $\Delta t \ll t$), and equation 23 may be further simplified to:

$$\dot{\epsilon} \approx A_3 \left(\frac{Gb}{kT} \right) \left[\sinh \left(\frac{\alpha\sigma}{G} \right) \right]^n D_{eff} \left\{ \left[\left(\frac{B_1 \gamma_s V_m C_o}{RT} \right) \bar{D}_{sol} (t + 2N \dot{\gamma} t_{hc} v_c \phi) + r_o^3 \right]^{1/3} \right\} \quad (24)$$

where the term within second brackets on the right hand side represents the particle size r following v_c cycles, given by:

$$r \approx \left\{ \left[\left(\frac{B_1 \gamma_s V_m C_o}{RT} \right) \bar{D}_{sol} (t + 2N \dot{\gamma} t_{hc} v_c \phi) + r_o^3 \right]^{1/3} \right\} \quad (25)$$

Note that for $\dot{\gamma} = 0$, r represents the coarsened size due to static aging only, whereas when $\dot{\gamma} \neq 0$, r includes contributions due to both static and strain-enhanced coarsening.

3. DISCUSSION

In equation 24, it is assumed that the particle size increment during the last part-cycle (i.e., Δr) is negligible compared to that achieved in the previous v_c cycles (i.e., r_{cum}), and that the particles grow incrementally at the end of each cycle. This assumption allows us to simplify the expression for the instantaneous particle radius r (equation 25), enabling us to plot r and hence $\dot{\epsilon}$ as functions of thermo-mechanical cycling at any given temperature. The constant A_3 is obtainable directly by fitting creep data for a constant

microstructure (r) to equation 4, B_1 (which depends on the second phase volume fraction V_f [15]) may be obtained by fitting static phase coarsening data to equation 8 after replacing the term $K_2 \cdot n_{\text{total}}$ by D_{sol} , and N is on the order of 100-1000, depending on the microstructural scale [15]. All other terms are either known or are estimable from first principles.

Figure 3 shows plots of equations 24 and 25 for a 150 μm diameter flip-chip solder joint situated at the corner of a 20mm square chip, and subjected to TMC between 223K and 413K, using values reasonable for 96.5Sn-3.5Ag solder. The initial second phase particle size was assumed to be 0.3 μm . To enunciate the effect of inelastic strain on coarsening, a plot of the particle size due to static coarsening only is also given. The values of the various parameters used in the calculations, some of which are directly obtained from the literature, and some of which are estimates, are listed in Table I. It is readily apparent that in agreement with experimental observations (Figure 2), the Ag_3Sn particle size coarsens rapidly during thermal cycling. The coarsening kinetics are significantly greater when inelastic strains are superimposed on the thermal cycle. It is also apparent that associated with the strain-enhanced coarsening, there is an appreciable increase in the creep rate at 400K. This trend is in general agreement with the results of ongoing impression creep experiments, which show that the measured creep rates can increase several-fold due to microstructural coarsening [19].

Equation 23 (or 24) constitutes the only available dislocation creep formulation incorporating the effect of second phase particle coarsening common in lead-free solders. The main advantages of the proposed model are as follows: (a) the closed-form of the proposed formulation allows *ease of incorporation* into existing finite element codes for joint reliability analysis; (b) since the law has built-in coarsening effects, it directly accounts for *local variations* in microstructural scale within a joint, which is influenced by the local strain history and stress state; (c) it *explicitly* accounts for the effects of prior strain history (ϵ_{cum}), the local hydrostatic stress state (σ_h), and the loading rate on the coarsening kinetics, and hence on creep; and (d) the first-principles based model *obviates the need for life-prediction approaches based on empirical dependencies* between microstructural scale and the number of cycles, which are strongly dependent on

experimental conditions. Follow-on work is necessary to: (a) experimentally determine the phenomenological constants in the creep and coarsening equations over a large range of σ/G and T/T_m for lead-free solders, and (b) validate the model experimentally.

4. SUMMARY

An approach is proposed for incorporating the effect of in-situ second-phase particle coarsening in a dislocation creep model applicable to lead-free solder alloys with a microstructure of finely dispersed intermetallics in a soft matrix. The formulation incorporates the effects of both static and strain-enhanced coarsening. It is shown that dispersed intermetallic particles in a lead-free solder alloy may undergo substantial strain-enhanced coarsening, and are subject to a commensurately increasing the creep rate, during TMC. The rigorous form of the proposed formulation allows step-wise updating of the creep behavior due to incremental coarsening during any time increment in the course of TMC of the solder joint. An approximate closed-form solution is also proposed, where the particle size, and hence the creep rate, is considered to increase only at the end of a complete thermal cycle. The formulations incorporate the effects of inelastic strain history and hydrostatic stress state, and can therefore allow different degrees of coarsening, with different resultant creep rates, at different locales inside a solder joint, when incorporated in numerical simulations (e.g., finite element models).

ACKNOWLEDGEMENTS

This work was conducted as part of the author's sabbatical at INTEL Corporation, Chandler, AZ. The author is grateful to Dr. Ravi Mahajan for offering him the sabbatical opportunity, and to Drs. George Raiser and Biju Chandran for their project mentorship. Thanks are also due to Drs. Darrel Frear and Jin-Wook Jang of Motorola for the many technical discussions on deformation of solder alloys, and making available samples of several lead-free solders with different thermo-mechanical histories.

REFERENCES :

1. W. Yang, R. W. Messler and L. E. Felton, "Microstructure Evolution of Eutectic Sn-Ag Solder Joints", *J. Electronic Mater.*, 1994, pp. 765-772.
2. S. Jin and M. McCormack, "Dispersoid Additions to a Pb-Free Solder for Suppression of Microstructural Coarsening", *J. Electronic Mater.*, 23, 1994, pp. 735-739.
3. M.L. Huang, C.M.L. Wu, J.K.L. Lai and Y.C. Chan, "Microstructural Evolution of a Lead-Free Solder Alloy Sn-Bi-Ag-Cu Prepared by Mechanical Alloying during Thermal Shock and Aging", *J. Electronic Mater.*, 29, 2000, pp. 1021-1361.
4. P. Hacke, A. F. Sprecher and H. Conrad, "Computer Simulation of Thermo-Mechanical Fatigue of Solder Joints Including Microstructure Coarsening", *J. Electronic Packg.*, 115, 1993, p. 153.
5. H. Conrad, Z. Guo, Y. Fahmy and D. Yang, "Influence of Microstructure Size on the Plastic Deformation Kinetics, Fatigue Crack Growth Rate and Low-Cycle Fatigue of Solder Joints", *J. Electronic Mater.*, 28, 1999, p. 1062.
6. D. Frear, S. Burchett, M. Neisen and J. Stephens, "Microstructurally Based Finite Element Simulation on Solder Joint Behavior", *Soldering & Surface Mount Tech.*, 25, 1997, p. 39.
7. P.T. Vianco, S.N. Burchett, M.K. Neilsen, J.A. Rejent and D.R. Frear, "Coarsening of the Sn-Pb Solder Microstructure in Constitutive Model Based Predictions of Solder Joint Thermal Mechanical Fatigue", *J. Electronic Mater.*, 28, 1999, p. 1290.
8. P.L. Hacke, Y. Fahmy and H. Conrad, "Phase Coarsening and Crack Growth Rate During Thermo-Mechanical Cycling of 63Sn37Pb Solder Joints", *J. Electronic Mater.*, 27, 1998, pp. 941-947.
9. R.W. Evans and B. Wilshire, "Creep of Metals and Alloys", *Inst. Metals, London*, 1985, p.104.
10. R. Darveaux and K. Banerji, *IEEE Trans. Comp. Hyb. Manuf. Technol.*, 15, 1992, p. 1013.
11. M. D. Matthew, S. Movva, H. Yang and K.L. Murty, in "Creep Behavior of Advanced Materials", R.S. Mishra, A.K. Mukherjee and K.L. Murty, eds., TMS, 1999, p. 51.

12. V.I. Igoshv and J. I. Kleiman, *J. Electronic Mater.*, 29, 2000, p. 244.
13. G. S. Ansell and J. Weertman, *Trans. Met. Soc. AIME*, 215, 1959, p. 838.
14. M.A. Clark and T.H. Alden, *Acta Met.*, 21, 1973, p. 1195.
15. O. N. Senkov and M. M. Myshlyaev, *Acta Met.*, 34, 1986, p. 97.
16. I. Dutta, A. Gopinath and C. Marshall, *J. Electronic Mater.*, 31, 2002, p. 253.
17. M. Lifshitz and V. Slyolov, *J. Phys. Chem. Solids*, 19, 1961, p. 35.
18. C. Wagner, *Z. Electrochem.*, 65, 1961, p. 581.
19. N. Anastasio and I. Dutta, unpublished research, Naval Postgraduate School.

TABLE I: Properties and constants used in calculationTMC parameters:

$$T_{\min} = 223\text{K}, T_{\max} = 413\text{K} (\Delta T = 190\text{K})$$

$$\Delta\alpha = 16 \times 10^{-6}/\text{K}$$

$$h = 150\mu\text{m} \text{ (total joint thickness including bond-pads : estimated to be } \sim \text{ball diameter)}$$

$$t_{\text{hc}} = 15 \text{ minutes}$$

$$x = \text{max. DNP} = 14\text{mm} \text{ (chip size } \sim 20\text{mm square)}$$

$$\phi \approx 0.9$$

Particle-coarsening parameters:

$$r_o = 0.3\mu\text{m}$$

$$V_f(\text{Ag}_3\text{Sn}) = 0.07$$

$$B_1 = 5 \times 10^{-3} \text{ m}^3/\text{moles}^2$$

$$\gamma = 0.5 \text{ J/m}^2$$

$$V_m(\text{Ag}_3\text{Sn}) \approx 1 \times 10^{-5} \text{ m}^3$$

$$C_o(\text{Ag in Sn}) \approx 20 \text{ moles/m}^3$$

$$N = 3000s$$

$$D_o^{\text{sol}} = 7 \times 10^{-7} \text{ m}^2/\text{s}$$

$$Q_{\text{sol}} = 51.5 \text{ kJ/mole}$$

$$\sigma_h \text{ (assumed constant)} = 10\text{MPa}$$

Creep Parameters [10]

$$T = 400\text{K}, \sigma = 10\text{MPa}$$

$$A_3 \left(\frac{b}{k} \right) D_o^{\text{eff}} = 6.66 \times 10^{-3} \frac{\text{m} - K}{N - s}$$

$$G(400\text{K}) = 10.54\text{GPa}$$

$$\alpha = 1300$$

$$n = 5.5$$

$$Q_{\text{eff}} = 39 \text{ kJ/mole}$$

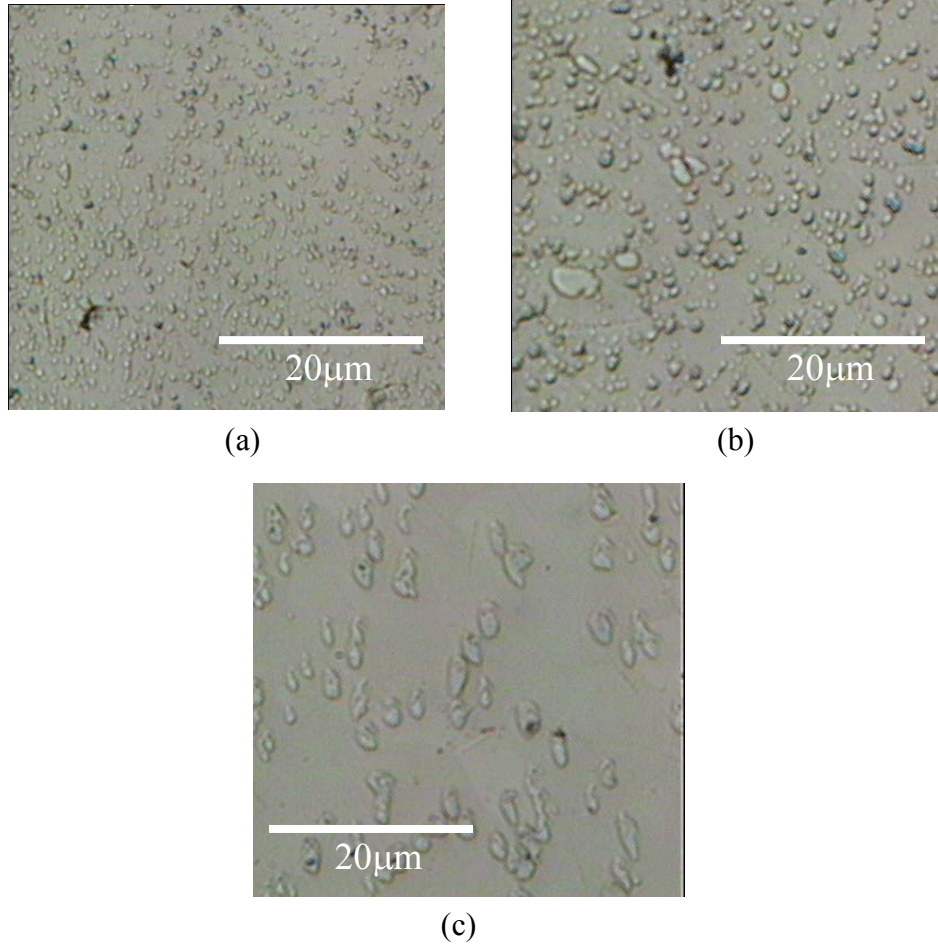


Figure 1: Microstructure of a flip-chip joint of Sn-4.7Ag-1.7Cu solder in the as re-flowed condition (a), and after 200 and 1200 TMCs (b and c, respectively) from -25°C to 125°C. The cycle period was 1 hour, with a nominal shear strain range of 0.1. The second phase particles are observed to coarsen significantly with progressive TMC.

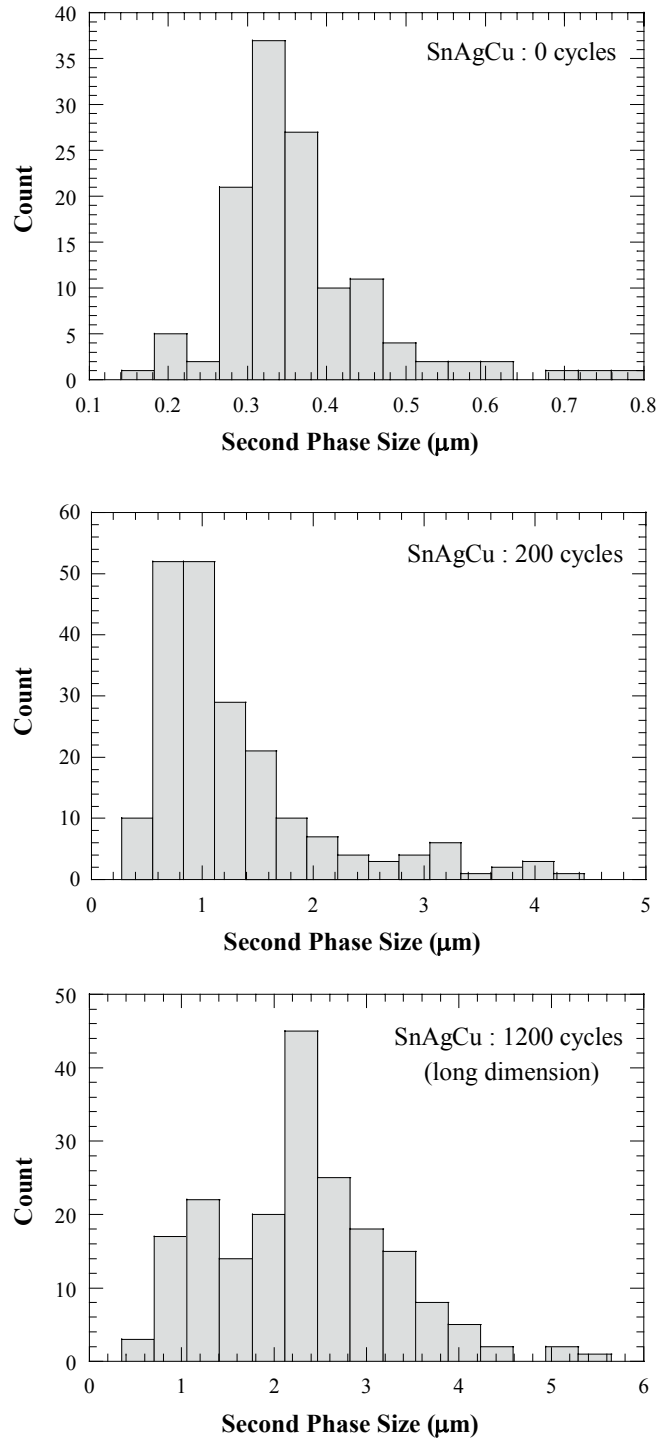


Figure 2: Size distribution of second phase particles in SnAgCu joints before and after thermo-mechanical cycling. Appreciable coarsening is noted during TMC.

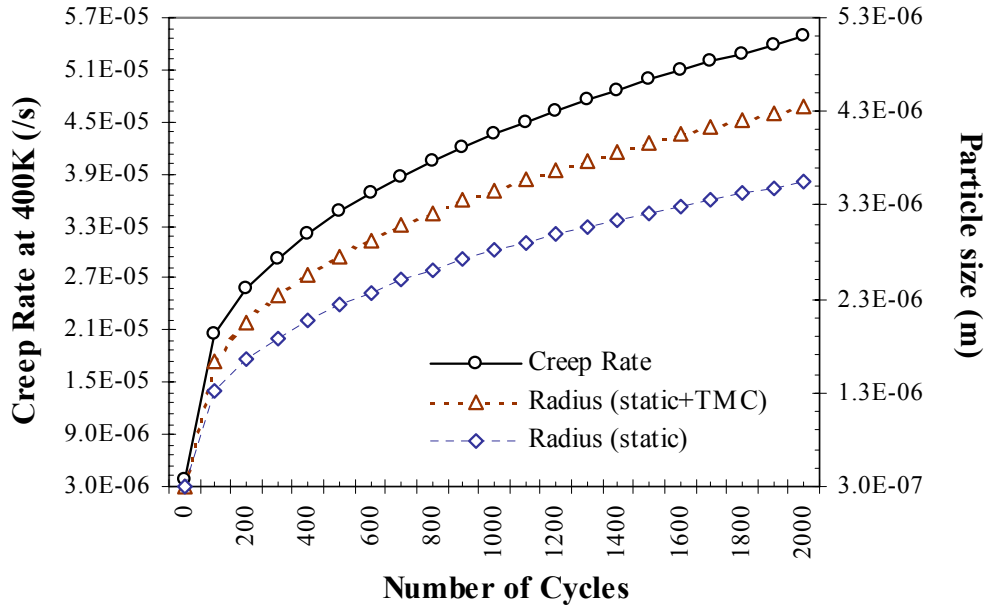


Figure 3: Computed increase in the Ag_3Sn particle size in eutectic Sn-Ag, and the associated increase in creep rate at 400K, during thermo-mechanical cycling between 223 and 413K with a period of 30 minutes/cycle. The contributions to coarsening from (a) static coarsening only, and (b) both static and strain-enhanced coarsening, are separately shown. The total imposed shear strain range during each half-cycle was assumed to be 0.287, corresponding to a typical flip-chip joint with a stand-off height of $150\mu\text{m}$, located at a DNP of 0.014m . During 2000 TMCs, a nearly fifteen-fold increase of particle radius, along with a commensurate enhancement of the solder creep response, is noted.